

Optimal Quantification of Contact Inhibition in Cell Populations

David J. Warne,¹ Ruth E. Baker,² and Matthew J. Simpson^{1,*}

¹School of Mathematical Sciences, Queensland University of Technology, Brisbane, Queensland, Australia and ²Mathematical Institute, University of Oxford, Oxford, United Kingdom

ABSTRACT Contact inhibition refers to a reduction in the rate of cell migration and/or cell proliferation in regions of high cell density. Under normal conditions, contact inhibition is associated with the proper functioning tissues, whereas abnormal regulation of contact inhibition is associated with pathological conditions, such as tumor spreading. Unfortunately, standard mathematical modeling practices mask the importance of parameters that control contact inhibition through scaling arguments. Furthermore, standard experimental protocols are insufficient to quantify the effects of contact inhibition because they focus on data describing early time, low-density dynamics only. Here we use the logistic growth equation as a caricature model of contact inhibition to make recommendations as to how to best mitigate these issues. Taking a Bayesian approach, we quantify the trade off between different features of experimental design and estimates of parameter uncertainty so that we can reformulate a standard cell proliferation assay to provide estimates of both the low-density intrinsic growth rate, λ , and the carrying capacity density, K , which is a measure of contact inhibition.

Contact inhibition is the tendency of cells to become nonmigratory and/or nonproliferative in regions of high cell density (1). The phenomena of contact inhibition of migration, involving processes such as adhesion, paralysis, and contraction (1), is distinct to contact inhibition of proliferation, driven by cell-cell signaling and adhesion (2,3); both phenomena are essential for the regulation of structure and function of multicellular organisms.

Down regulation of contact inhibition of proliferation enhances tumor spreading (4), while wound healing and tissue regeneration also depend crucially on contact inhibition of proliferation (5). Although contact inhibition of proliferation is ubiquitous in both normal and pathological processes, it is difficult to quantify the impact of such contact inhibition in complex biological systems despite the availability of experimental data. Therefore, mathematical models have an important role in informing our understanding of how contact inhibition of proliferation affects collective cell behavior.

The most fundamental mathematical model describing contact inhibition of cell proliferation is the logistic growth model (6–9),

$$\frac{dC(t)}{dt} = \underbrace{\lambda C(t)}_{\text{proliferation}} \times \underbrace{\left[1 - \frac{C(t)}{K}\right]}_{\text{contact inhibition}}, \quad (1)$$

where $C(t) > 0$ is the cell density at time t , $\lambda > 0$ is the proliferation rate, and $K > 0$ is the carrying capacity density. The carrying capacity density is the density at which contact inhibition decreases the net growth rate to zero. The logistic growth model is used ubiquitously in the study of development, repair, and tissue regeneration, including for the modeling of tumor growth (10–13) and wound healing (6,14,15). The solution of Eq. 1,

$$C(t) = \frac{C(0)K}{[(K - C(0))\exp(-\lambda t) + C(0)]}, \quad (2)$$

is a sigmoid curve that increases from $C(t) = C(0)$ to $C(t) = K$ as $t \rightarrow \infty$, provided that $C(0)/K \ll 1$.

In vitro cell proliferation assays are used routinely to examine mechanisms that control cell proliferation, such as the application of various drugs and other treatments on the rate of cell proliferation (16,17). In vitro assays are routinely used to inform the development and interpretation of in vivo assays describing pathological situations, such as tumor growth (18). Therefore, improving the design and interpretation of in vitro assays will have an indirect influence on the way that we design and interpret in vivo assays.

Submitted July 17, 2017, and accepted for publication September 15, 2017.

*Correspondence: matthew.simpson@qut.edu.au

Editor: Stanislav Shvartsman.

<https://doi.org/10.1016/j.bpj.2017.09.016>

© 2017 Biophysical Society.

A cell proliferation assay typically involves placing cells, at low density, $C(0)/K \ll 1$, onto a 2D surface and reexamining the increased monolayer density at a later time, $t = T$. Typical data from a cell proliferation assay are given in Fig. 1, A and B.

To use Eq. 1 to quantitatively inform our understanding of a particular biological system, we must be able to estimate the initial density, $C(0)$, and the model parameters, λ and K . Obtaining an accurate estimate of K is crucial to understand how contact inhibition controls net the proliferation rate at modest to high densities. However, despite the importance of K , most theoretical studies work with a nondimensionalized model by setting $c(t) = C(t)/K$. This leads to (6,7,14)

$$\frac{dc(t)}{dt} = \lambda c(t)[1 - c(t)],$$

which completely masks the importance of being able to accurately estimate the carrying capacity, K .

Not only do standard mathematical approaches prevent quantitative assessment of the impact of contact inhibition, standard experimental protocols for in vitro proliferation assays are also insufficient to estimate K . Very recently, Jin et al. (19) used Eq. 1 to analyze a set of cell proliferation assays performed with a prostate cancer cell line, and concluded that standard experimental data do not lead to robust, biologically relevant estimates of K . This is consis-

tent with the work of Sarapata and de Pillis (20) who also find that standard in vitro experimental data are insufficient to estimate K using best-fit, nonlinear least-squares methods. The fundamental issue, as illustrated in Fig. 1 C, is that cell proliferation assays are initiated with a small density and performed for a relatively short duration. This strategy is sufficient for estimating the low-density intrinsic proliferation rate, λ , but completely inadequate for estimating K , which is associated with longer time, higher density data. Given the importance of K , we are motivated to reconsider the design of proliferation assays so that we can quantitatively estimate both λ and K from a single experiment.

The typical duration of a proliferation assay is less than 24 h (16), with some assays as short as 4 h (21), and the cell density is recorded once, at the end point of the experiment. This timescale is sufficient to estimate the low-density intrinsic proliferation rate, λ , because the doubling time of the majority of cell lines is approximately 24 h (6,7,13,15). However, this standard timescale is far too short to robustly quantify contact inhibition effects given the low initial densities that are routinely used. For example, the PC-3 prostate cancer cell line examined by Jin et al. (19) proliferates with $\lambda \approx 0.05/\text{h}$, but on the timescale of the experiment the observed growth of the population is approximately exponential. This is consistent with Eq. 1 because we have $C(t) \sim C(0) \exp(\lambda t)$, provided that $C(0)/K \ll 1$, and t is sufficiently small. Fig. 1 C shows that the early time growth dynamics are effectively independent of K , confirming that it is impossible to obtain robust estimates of K using standard data (19,20).

The aim of this work is to provide guidance about how to overcome these standard experimental and theoretical limitations by taking a Bayesian approach to experimental design (22–27). The advantage of taking a Bayesian approach is that we have a platform to quantitatively examine how the uncertainty in our estimate of K depends on the experimental design: we aim to provide guidance for experimental design that minimizes the uncertainty in our estimate of K . To achieve this, we consider a proliferation assay of duration T , with n observations of cell density, $C_{\text{obs}}^{1:n} = [C_{\text{obs}}(t_1), \dots, C_{\text{obs}}(t_n)]$, at times t_1, \dots, t_n with $0 < t_i \leq T$ for all $i = [1, \dots, n]$. These data could represent a single experiment observed at multiple time points, $t_1 < t_2 < \dots < t_n < T$, or n identically prepared experiments, each of which is observed once, $t_1 = t_2 = \dots = t_n = T$. We assume that cells proliferate according to Eq. 1 with known λ and $C(0)$. Furthermore, we assume $C(0)/K \ll 1$. Our assumption that λ can be determined is reasonable because $C(t) \sim C(0)\exp(\lambda t) = C(0)[1 + \lambda t + O(t^2)]$ for $C(0)/K \ll 1$. This means that fitting a simple straight line or exponential curve to typical experimental data will provide a reasonable estimate of λ . The assumption that $C(0)$ is known precisely is less realistic. For example, estimates of $C(0)$ are affected profoundly by fluctuations in the initialization of the experiment as proliferation assays are performed by placing a known number of cells onto a tissue culture plate. However, images of the experiments are obtained

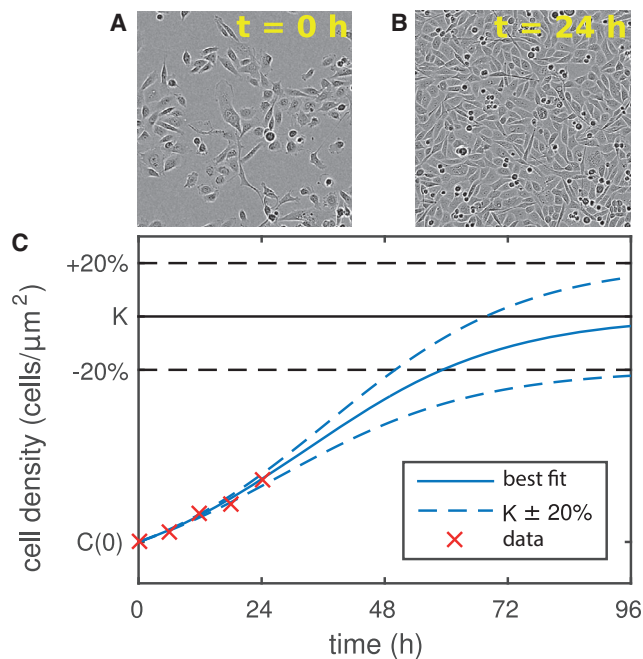


FIGURE 1 Proliferation assay using a prostate cancer cell line. Images of area $450 \mu\text{m}^2$ are captured at (A) $t = 0$ h and (B) $t = 24$ h. Images are reproduced from Jin et al. (19), with permission. (C) Logistic growth curve with $C(0) = 3.1 \times 10^{-4}$ (cells/ μm^2), $\lambda = 0.052$ (1/h), and $K = 2 \times 10^{-3}$ (cells/ μm^2) (solid black). Additional solutions with $K \pm 20\%$ (dashed black) also fit the short time experimental data (red crosses).

over a much smaller spatial scale. This means that the role of stochastic fluctuations can be significant (19).

To make progress, we assume that observations are made, and are subject to Gaussian-distributed experimental measurement error with zero mean and variance Σ^2 . Under these conditions, our knowledge of the carrying capacity, K , given such observations, is represented by the probability density function

$$p(K | C_{\text{obs}}^{1:n}) = A \prod_{i=1}^n \phi[C_{\text{obs}}(t_i); C(t_i), \Sigma^2], \quad (3)$$

where A is a normalization constant and $\phi[\cdot; C(t_i), \Sigma^2]$ denotes a Gaussian probability density with mean $C(t_i)$ and variance Σ^2 (Supporting Material). This probability density represents knowledge obtained from the data when no prior assumptions are made on K . The point of maximum density in Eq. 3 corresponds to the maximum likelihood estimator or best-fit estimate, \hat{K} . Importantly, Eq. 3 also enables the quantification of uncertainty in this estimate through calculation of the variance,

$$\sigma_n^2 = \int_0^\infty (K - \hat{K})^2 p(K | C_{\text{obs}}^{1:n}) dK. \quad (4)$$

Fig. 2 A shows the probability density of K (Eq. 3) for several values of T for the typical assay protocol where only a single observation is made ($n = 1$). Here, our estimates of λ , $C(0)$, and Σ are based on reported values (19). The spread of these curves indicates the degree of uncertainty in any estimate of K . In particular, note the red line, which indicates the probability density for K for a measurement taken at the standard duration of $T = 24$ h. The relatively flat, disperse nature of the profile confirms that standard proliferation assay designs are completely inappropriate to estimate K because the profile lacks a well-defined maximum. This result provides a formal explanation for the observations of both Sarapata and de Pillis (20) and Jin et al. (19). In response to this issue, here we provide quantitative guidelines about how the experimental design can be chosen to facilitate accurate quantification of the effects of contact inhibition.

One optimistic assumption in Eq. 3 is the supposition that $C(0)$ is known precisely. In reality, $C(0)$ is subject to both measurement errors and systematic errors owing to stochastic fluctuations (19). We extend our analysis to incorporate uncertainty in the estimate of $C(0)$ by also assuming $C(0)$ to be Gaussian-distributed with mean μ_0 and variance Σ_0^2 , that is $p[C(0)] = \phi[C(0); \mu_0, \Sigma_0^2]$. In this case, Eq. 3 generalizes to (Supporting Material)

$$p(K | C_{\text{obs}}^{1:n}, \mu_0, \Sigma_0^2) = \int_0^\infty p(K | C_{\text{obs}}^{1:n}) p[C(0)] dC(0). \quad (5)$$

The integral in Eq. 5 is intractable, so numerical integration is required to evaluate $p(K | C_{\text{obs}}^{1:n}, \mu_0, \Sigma_0^2)$.

Because $C(t_i) \rightarrow K$ as $t_i \rightarrow \infty$ for all $i = 1, 2, \dots, n$, then, for both Eqs. 3 and 5, we obtain (Supporting Material)

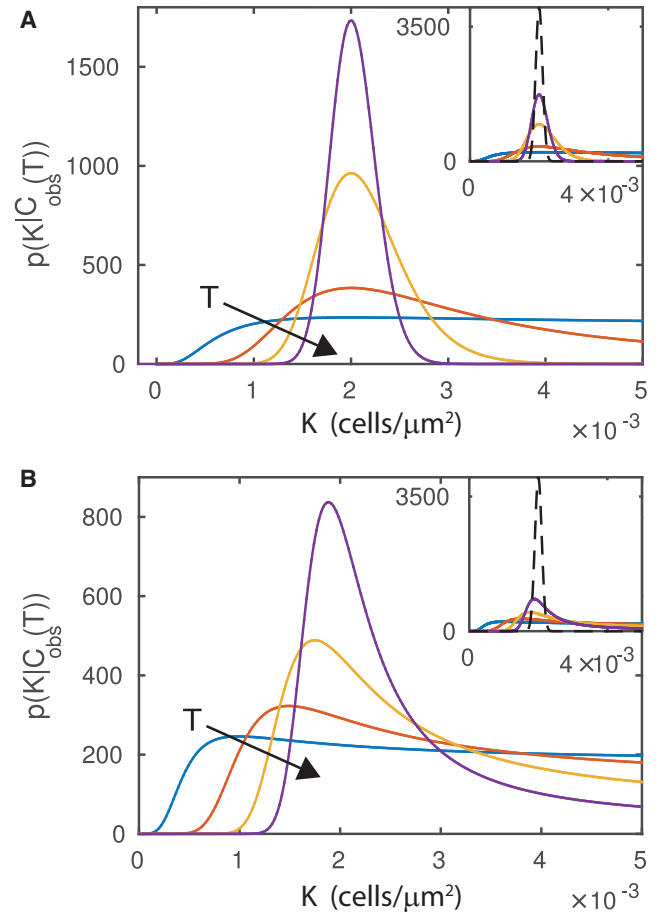


FIGURE 2 The probability density, $p(K | C_{\text{obs}}^{1:n})$, with $n = 1$ plotted for $T = 12$ h (black), 24 h (red), 36 h (yellow), and 48 h (purple), where $\lambda = 5.2 \times 10^{-2}$ (1/h), $\Sigma = 10^{-4}$ (cells/ μm^2), and the true carrying capacity is $K = 2 \times 10^{-3}$ (cells/ μm^2). (A) The initial density, $C(0)$, is assumed to be known precisely, $C(0) = 3.1 \times 10^{-4}$ (cells/ μm^2). (B) This includes uncertainty in the initial condition with $\mu_0 = 3.1 \times 10^{-4}$ (cells/ μm^2) and $\Sigma_0 = 1.02 \times 10^{-4}$ (cells/ μm^2). The insets in both (A and B) show the main plot in the context of the limiting density as $T \rightarrow \infty$ (black dashed line).

$$\lim_{(t_1, \dots, t_n) \rightarrow (\infty, \dots, \infty)} p(K | C_{\text{obs}}^{1:n}) = \phi\left(K; \frac{1}{n} \sum_{i=1}^n C_{\text{obs}}^i, \frac{\Sigma^2}{n}\right). \quad (6)$$

Fig. 2 A demonstrates that the probability density function for K , Eq. 3, tightens toward the limiting density, Eq. 6, as T increases. Note that for the typical assay duration, $T < 24$ h, the density is approximately uniform. Again, this reiterates the fact that standard experimental designs are inadequate to characterize the effects of contact inhibition, and that different approaches are required. The effect of uncertainty in $C(0)$ is clear in Fig. 2 B. Even with $T = 48$ h, there is a very large region of nonzero, near-constant probability density, indicating very wide confidence intervals for the estimate of K . Equation 6 also provides a lower bound on the uncertainty in the estimate of K ,

$$\sigma_n^2 \geq \frac{\Sigma^2}{n}, \quad (7)$$

for any choice of $C(0)$ and λ . This result is independent of the treatment of the uncertainty in $C(0)$, but requires observations to be made after an infinite duration of time.

Equations 6 and 7 tell us two important things about assay design in the study of contact inhibition. First, there is a fundamental lower bound on the uncertainty in our estimate of K for a fixed number, n , of observations of the density. However, increasing the assay duration, T , always provides more information. Second, increasing the number of observations, n , always provides more information and, further, it decreases the long time lower bound on the uncertainty in the estimate of K . Hence, Eq. 7 informs the minimum number of observations required to estimate K accurately.

Clearly, practical experimental designs require finite T , so we require methods to determine T such that the uncertainty in K is sufficiently close to the lower bound. We can quantify, for the standard choice of $n = 1$, the approximate uncertainty in our estimate of K (Supporting Material) (28), given by

$$\sigma_1^2 = \frac{C(0)^4 [1 - \exp(-\lambda T)]^2}{[C(0) - C_{\text{obs}}(T) \exp(-\lambda T)]^4} \Sigma^2. \quad (8)$$

This estimate of the uncertainty in K is accurate, provided $C_{\text{obs}}(T)/\Sigma^2 \gg 1$. This expression provides a practical tool to assess the information content of data, but also enables one to estimate whether T is large enough that the uncertainty in K is sufficiently close to the lower bound (Supporting Material).

Equation 7 gives us a method of quantifying the information gained by introducing more observations into the idealized case that T is sufficiently large. For example, doubling n will half the uncertainty. However, because practical limitations mean that T is finite, this result does not always hold. Fig. 3 A shows that the effect of doubling n varies significantly, depending on the choice of T . Here, the n observations are taken at regular intervals. For example, if $T < 1/\lambda$, increasing n has almost no effect on the uncertainty, σ_n^2 . There is a similar negligible effect for $T > -1/\lambda \log C(0)/[K - C(0)]$, which is the time corresponding to the point of inflection of Eq. 2.

These results highlight several subtle, but immensely important considerations. For example, at sufficiently short times, increasing n has very little benefit. Similarly, at sufficiently large times increasing T has little benefit. The most useful result is that for intermediate times there is more value in increasing T than in increasing n . Furthermore, if we wish to go beyond the standard experimental design where a single measurement is made at the end of the experiment, $t = T$, we might want to quantify the benefit of making a second observation at an earlier time, $t < T$, during the same experiment. In this scenario, results in Fig. 3

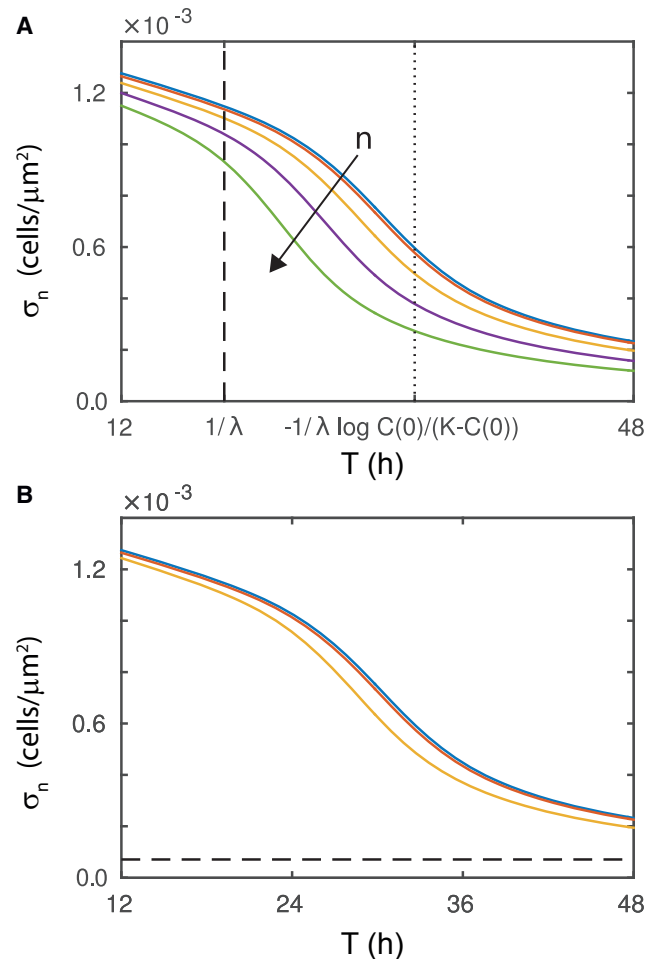


FIGURE 3 (A) Uncertainty in K as a function of T for $n = 1$ (black), $n = 2$ (red), $n = 4$ (yellow), $n = 8$ (purple) and $n = 16$ (green); here, observations are taken at regular intervals. (B) Effect of observation placement is given for $n = 2$ with $t_2 = T$, $t_1 = T/5$ (black), $t_1 = T/2$ (red), and $t_1 = 4T/5$ (yellow). The lower bound on uncertainty, σ_n is given for $n = 2$ (dashed). The uncertainty, σ_n is calculated using the trapezoid rule with 10^5 equally spaced panels over the interval $0 < K < 5 \times 10^{-3}$ (cells/ μm^2).

B show that the choice of time at which the second measurement is made can be important. Comparing Fig. 3 A with Fig. 3 B shows that a poor choice of the time for the second observation might not lead to any more change than simply taking a single observation at T . However, selecting two well-placed observation times can be as informative as making four equally spaced observations.

We conclude by providing several guidelines for the design of cell proliferation assays:

- 1) Reducing the uncertainty in $C(0)$ is crucial, especially if $T < 48$ h;
- 2) Equation 8 should be used with short timescale data to estimate the smallest value of T that will result in acceptable uncertainty in K ; and
- 3) On a short timescale, increasing T is more informative than increasing n . However, if increasing T is infeasible,

the optimal strategy is to repeat the experiment n times and make n observations at time T . In many situations, n will need to be large to account for the short timescale. Fig. 3 A shows that even a 16-fold increase in n is still unacceptable for $T < 12$.

In this work, we highlight certain aspects of assay design that are often neglected and unreported. However, these features are critical if we are to quantify the role of crowding and contact inhibition of proliferation in populations of cells. The guidelines we propose allow us to provide the best estimates of λ and K using a single experiment, whereas standard experimental designs allow us to confidently estimate λ only. Our results confirm that standard in vitro experimental designs are well suited for estimating λ , but poorly suited for estimating K . A different approach is required to overcome this limitation, and here we provide quantitative guidance about designing in vitro proliferation assays that can be used to estimate both λ and K . The situation is even more complex for in vivo assays in which there are more experimental constraints and unknowns. However, improving the way that we design and interpret in vitro assays is relevant because these simpler experiments are routinely used in tandem with in vivo assays due to the fact that they are cheaper and faster to perform than working in live tissues.

SUPPORTING MATERIAL

Supporting Materials and Methods and one table are available at [http://www.biophysj.org/biophysj/supplemental/S0006-3495\(17\)31028-7](http://www.biophysj.org/biophysj/supplemental/S0006-3495(17)31028-7).

AUTHOR CONTRIBUTIONS

D.J.W., R.E.B., and M.J.S. designed the research. D.J.W. performed the research. D.J.W., R.E.B., and M.J.S. contributed analytic tools. D.J.W., R.E.B., and M.J.S. analyzed the data. D.J.W., R.E.B., and M.J.S. wrote the article.

ACKNOWLEDGMENTS

We thank Michael Stumpf and two anonymous referees for helpful comments. We also thank the HPC and Advanced Research Computing support at QUT for computational resources.

M.J.S. thanks the Australian Research Council (DP170100474). R.E.B. thanks the Royal Society for a Royal Society Wolfson Research Merit Award, and the Leverhulme Trust for a Leverhulme Research Fellowship.

REFERENCES

1. Abercrombie, M. 1970. Contact inhibition in tissue culture. *In Vitro*. 6:128–142.
2. Levine, E. M., Y. Becker, ..., H. Eagle. 1965. Contact inhibition, macromolecular synthesis, and polyribosomes in cultured human diploid fibroblasts. *Proc. Natl. Acad. Sci. USA*. 53:350–356.
3. Liu, L., B. Sun, ..., R. H. Austin. 2011. Probing the invasiveness of prostate cancer cells in a 3D microfabricated landscape. *Proc. Natl. Acad. Sci. USA*. 108:6853–6856.
4. Abercrombie, M. 1979. Contact inhibition and malignancy. *Nature*. 281:259–262.
5. Puliafito, A., L. Hufnagel, ..., B. I. Shraiman. 2012. Collective and single cell behavior in epithelial contact inhibition. *Proc. Natl. Acad. Sci. USA*. 109:739–744.
6. Maini, P. K., D. L. S. McElwain, and D. I. Leavesley. 2004. Traveling wave model to interpret a wound-healing cell migration assay for human peritoneal mesothelial cells. *Tissue Eng*. 10:475–482.
7. Maini, P. K., D. L. S. McElwain, and D. I. Leavesley. 2004. Travelling waves in a wound healing assay. *Appl. Math. Lett.* 17:575–580.
8. Treloar, K. K., M. J. Simpson, ..., R. E. Baker. 2014. Are in vitro estimates of cell diffusivity and cell proliferation rate sensitive to assay geometry? *J. Theor. Biol.* 356:71–84.
9. Tsoularis, A., and J. Wallace. 2002. Analysis of logistic growth models. *Math. Biosci.* 179:21–55.
10. Enderling, H., and M. A. J. Chaplain. 2014. Mathematical modeling of tumor growth and treatment. *Curr. Pharm. Des.* 20:4934–4940.
11. Gerlee, P. 2013. The model muddle: in search of tumor growth laws. *Cancer Res.* 73:2407–2411.
12. Scott, J. G., D. Basanta, ..., P. Gerlee. 2013. A mathematical model of tumour self-seeding reveals secondary metastatic deposits as drivers of primary tumour growth. *J. R. Soc. Interface.* 10:20130011.
13. Treloar, K. K., M. J. Simpson, ..., R. E. Baker. 2013. Multiple types of data are required to identify the mechanisms influencing the spatial expansion of melanoma cell colonies. *BMC Syst. Biol.* 7:137.
14. Sherratt, J. A., and J. D. Murray. 1990. Models of epidermal wound healing. *Proc. Biol. Sci.* 241:29–36.
15. Simpson, M. J., B. J. Binder, ..., R. E. Baker. 2013. Experimental and modelling investigation of monolayer development with clustering. *Bull. Math. Biol.* 75:871–889.
16. Chen, K., Q. Liu, ..., X. Jiang. 2017. Human MSCs promotes colorectal cancer epithelial-mesenchymal transition and progression via CCL5/ β -catenin/Slug pathway. *Cell Death Dis.* 8:e2819.
17. Delarue, M., F. Montel, ..., G. Cappello. 2014. Compressive stress inhibits proliferation in tumor spheroids through a volume limitation. *Biophys. J.* 107:1821–1828.
18. Beaumont, K. A., N. Mohana-Kumaran, and N. K. Haass. 2013. Modeling melanoma in vitro and in vivo. *Healthcare (Basel)*. 2:27–46.
19. Jin, W., E. T. Shah, ..., M. J. Simpson. 2017. Logistic proliferation of cells in scratch assays is delayed. *Bull. Math. Biol.* 79:1028–1050.
20. Sarapata, E. A., and L. G. de Pillis. 2014. A comparison and catalog of intrinsic tumor growth models. *Bull. Math. Biol.* 76:2010–2024.
21. Huang, F.-T., W. Y. Chen, ..., S.-N. Zhang. 2017. The novel long intergenic noncoding RNA UCC promotes colorectal cancer progression by sponging miR-143. *Cell Death Dis.* 8:e2778.
22. Gelman, A., J. B. Carlin, ..., D. B. Rubin. 2014. Bayesian Data Analysis. CRC Press, Boca Raton, FL.
23. Liepe, J., S. Filippi, ..., M. P. H. Stumpf. 2013. Maximizing the information content of experiments in systems biology. *PLoS Comput. Biol.* 9:e1002888.
24. Silk, D., P. D. W. Kirk, ..., M. P. H. Stumpf. 2014. Model selection in systems biology depends on experimental design. *PLoS Comput. Biol.* 10:e1003650.
25. Vanlier, J., C. A. Tiemann, ..., N. A. W. van Riel. 2012. A Bayesian approach to targeted experiment design. *Bioinformatics*. 28:1136–1142.
26. Vanlier, J., C. A. Tiemann, ..., N. A. W. van Riel. 2014. Optimal experiment design for model selection in biochemical networks. *BMC Syst. Biol.* 8:20.
27. Browning, A. P., S. W. McCue, and M. J. Simpson. 2017. A Bayesian computational approach to explore the optimal duration of a cell proliferation assay. *Bull. Math. Biol.* 79:1888–1906.
28. Ang, A., and W. H. Tang. 2007. Probability Concepts in Engineering. Wiley, New York.